Sensors & Actuators: B. Chemical 425 (2025) 136984

Contents lists available at ScienceDirect

Sensors and Actuators: B. Chemical

journal homepage: www.elsevier.com/locate/snb

Sulfur poisoning of powder aerosol deposited films of $BaFe_{0.74}Al_{0.01}Ta_{0.25}O_{3-\delta}$: A material for resistive temperature independent oxygen sensors

Carsten Steiner, Gunter Hagen, Ralf Moos *

Department of Functional Materials, Center of Energy Technology (ZET), University of Bayreuth, Bayreuth 95447, Germany

ARTICLE INFO

Keywords:
Gas sensors
Sulfur dioxide
Poisoning
Oxygen sensor
Air-fuel ratio
Exhaust gas

ABSTRACT

Barium-iron-aluminum-tantalate (BFAT) is a promising candidate for resistive oxygen sensors with temperature independent sensor characteristics for exhaust gas purposes. To evaluate the long-term stability of the dense sensor films that were prepared by powder aerosol deposition (PAD), this study investigates sulfur dioxide (SO_2) poisoning and its effect on the sensor characteristics. The results show that exposure to SO_2 significantly affects the electrical properties of the film material. After contact to SO_2, the resistance of BFAT heavily increases by about one decade and the oxygen sensitivity of the sensor element decreases. In addition, the selectivity is also negatively affected. Despite fresh sensors are nearly unaffected by interfering compounds, cross-sensitivities for poisoned sensors, appear, primarily towards nitrogen dioxide (NO_2), ammonia (NH_3), and to a lesser extent also towards other gases, that may be present in typical exhausts. X-ray diffraction (XRD) patterns of the poisoned powder and X-ray photoelectron spectroscopy (XPS) of the BFAT film confirmed the formation of $BaSO_4$, which also suggests that other reaction products may be generated during poisoning. Based on the experimental results, some ideas on the poisoning mechanism are discussed. The regeneration of a sulfur poisoned sensor element at high temperatures is only partially possible under oxidizing conditions, but it can provide a limited recovery of the BFAT resistance, sensitivity, and selectivity. In agreement with literature, these conditions will probably allow the removal of surface adsorbed sulfates only, while crystalline $BaSO_4$ is hardly removed. Overall, the material's resistance to sulfur dioxide poisoning remains a challenge that needs to be solved.

1. Introduction

In the past, several materials have been introduced for resistively measuring the oxygen partial pressure (pO_2) in exhaust gases. In this regard sensors films made from metal oxides were widely studied in the research community [1–12]. Particular attention has been paid to those metal oxides, whose electrical resistivity is independent of temperature. One of the first representatives developed in the last decades were sensors based on $SrTi_{1-x}Fe_xO_{3-\delta}$ (STF) [5,13,14]. However, materials such as $Co_{1-x}Mg_xO$ [15], $SrTi_{1-x}Mg_xO_3$ [16] and La_2CuO_4 [17] and others [18] also have low thermal activation energies.

$BaFe_{1-x}Al_{0.01}Ta_xO_{3-\delta}$ (BFAT) shows also temperature independent properties at a tantalum concentration of around $x = 25$ % [4,19–22]. Like in other materials of this family, the low temperature coefficients of BFAT are achieved by adjusting of its defect chemistry to minimize the thermal impact on the electrical resistivity [23]. The temperature-independent properties of BFAT have been demonstrated in previous studies, particularly on nanocrystalline sensor films prepared by powder aerosol deposition (PAD), a powder spray coating technique that is also known as aerosol deposition method (ADM). BFAT sensor films are therefore suitable as resistive oxygen sensors [24] and provide good selectivity to oxygen [19]. Experiments in engine exhaust gas have already shown that the material is suitable for determining the oxygen stoichiometry λ of engines with excess of oxygen (diesel) [19,25], which is defined by.

$$\lambda = \frac{\text{supplied air volume}}{\text{stoichiometrically required air volume}} \quad (1\text{-}1)$$

The oxygen stoichiometry can be derived from pO_2 by [26]. Beyond measuring oxygen concentration, BFAT sensor films have also been integrated into sensor concepts for the simultaneous determination of different gas concentrations (so-called multigas sensors) and have been

* Corresponding author.
E-mail address: functional.materials@uni-bayreuth.de (R. Moos).

https://doi.org/10.1016/j.snb.2024.136984
Received 9 September 2024; Received in revised form 24 October 2024; Accepted 20 November 2024
Available online 22 November 2024

successfully tested in engine exhaust gases of typical driving cycles [25]. However, the sulfur resistance of gas sensors is important for their long-term stability and was proven to be critical in some cases. The electrical resistance of STF films, for example, increased significantly during exposure to SO_2 due to the formation of $SrSO_4$ [27]. Approaches such as the integration of sulfur-absorbing top films may offer solutions to this problem [28].

The influence of sulfur poisoning on alkaline earth materials, especially Ba, has also been known for some time. Numerous studies in the early 2000s on Ba-based NO_x storage catalysts (NSC) with noble metals (mostly $Pt/BaO/Al_2O_3$) showed that the NO_x storage capacity is significantly reduced by the formation of barium sulfates [29–31]. Regeneration, i.e., removal of the sulfates, is partially possible under reducing conditions and at elevated temperatures [32–34], but leads to premature thermal aging of the catalyst [35]. Sulfates in the vicinity of precious metals and adsorbed amorphous sulfate compounds can be largely removed during regeneration. In contrast, the removal of bulk sulfates is hardly possible, but they also contribute significantly to the loss of NO_x storage capacity [36].

As an alternative to $Pt/BaO/Al_2O_3$ catalysts Ba-based perovskite catalysts have also been considered in the past [37–40]. The sulfur resistance is highly dependent on the perovskite composition and structural homogeneity [41]. Among these, BaFe perovskites are largely resistant to sulfur poisoning [38,41]. The combination of Ba and Fe was also considered because the addition of Fe has already been shown to be beneficial in $Pt/BaO/Al_2O_3$ catalysts. In this context, iron inhibits the grain growth of sulfates and also reduces the regeneration temperature [30,41,42]. An even higher resistance to sulfur has been found for $BaFe_{1-x}Ti_xO_{3-\delta}$ perovskite catalysts [38].

For the barium-iron-aluminum-tantalate ($BaFe_{1-x}Al_{0.01}Ta_xO_{3-\delta}$) PAD films, analyses on the effects of sulfur dioxide poisoning (also in the context of sensor applications) are still lacking. Even though the previous studies may provide some insights into expected mechanisms, a direct transfer of the results from Ba-based NO_x storage catalysts is difficult because many conditions are fundamentally different: First, sulfur poisoning has not yet been explicitly investigated for barium-iron-tantalate family. Secondly, the typical operating temperatures of the sensor (min. 600 °C) are at the upper end of the operating window for classical LNT (lean NO_x trap) applications. At the same time, analyses on the LNT are primarily aimed at the catalytic activity and the (NO_x) storage properties, while on the sensor film, the defect-chemical interaction with oxygen and its influence on the electrical properties of the material is decisive. Third, compared to typical catalyst applications, there are no dispersed precious metal-contacts on the surface, which (as mentioned above) have been shown to influence the (de)sulfation chemistry. And last but not least, the morphology of the materials also differs strongly due to their intended use: while nanostructured washcoats with a high surface area are used for NSC, the BFAT film is also nanocrystalline, but a dense ceramic film.

For all these reasons, a separate investigation of the effect of sulfur dioxide on the sensor material is necessary, which will be done in this study. The main focus will be on the sensing properties. Therefore, the effects of sulfur poisoning on the electrical resistance, on oxygen sensitivity, and on selectivity towards oxygen will be analyzed. In addition, the poisoning mechanisms will be investigated shortly from a materials perspective and the effects of poisoning on defect chemistry will be discussed. Based on the experimental findings, some ideas about the poisoning mechanism will be presented. In part, the results will also be compared to the performance of STF in order to generally classify the sulfur resistance compared to an alternative material for temperature-independent resistive oxygen sensors.

2. Materials and methods

2.1. Sensor preparation

Several analyses are presented in this study, beginning with a brief explanation of the scope and key ideas of our approach: In a first step, the prepared sensors were poisoned with SO_2 at different, application-relevant temperatures (600 °C and 800 °C). The focus of this and further investigations is the analysis of the electrical properties of the BFAT sensor characteristics. In order to investigate whether a (partial) regeneration of the sensor properties is possible at high temperatures, one of the sensors poisoned at 600 °C was then thermally treated at 900 °C in a chamber furnace (air atmosphere). The sensors were then tested in synthetic gas mixtures to determine their sensitivity to the oxygen partial pressure pO_2.The selectivity of the sensor elements, i.e., their cross-sensitivity to other gases, was also analyzed. These results were compared with the properties of fresh sensors. Finally, poisoned BFAT sensor films were investigated with X-ray diffraction (XRD) and X-ray photoelectron spectroscopy (XPS). Before going into the details of the individual experiments, the preparation of the sensor is described in the following:

The $BaFe_{0.74}Al_{0.01}Ta_{0.25}O_{3-\delta}$ perovskite was synthesized via the mixed oxide route previously described in [19,43]. The synthesized powder was sieved with a 200 μm mesh to remove larger agglomerates. The deposition was carried out by powder aerosol deposition (PAD) [22,44], as this is the only deposition method that reproducibly provides temperature independent sensor characteristics. The process uses oxygen as the carrier gas. The sensor film is deposited on an alumina substrate with screen-printed Pt electrodes to measure the 4-wire resistance. The process parameters of the PAD follow the specifications of [21,43]. As in previous studies, a thickness of ca. 5 μm was confirmed for dense ceramic sensor films by scanning electron microscopy (SEM). Close-up images of the sensor films are not included in this manuscript but can be found in [19,43], for example. The complete sensor layout is shown in Fig. 1a. A Pt heater structure (4-wire) is applied to the reverse side of the sensor element. As recommended in [19], the sensors were then annealed in air in a chamber furnace at 900 °C for 20 min to relax the lattice structure and restore the electrical properties.

2.2. Experimental section

The experiments for sensor poisoning were carried out in synthetic gas atmospheres with actively heated sensor elements, which are mounted in a housing (Fig. 1b). In the vertically oriented sensor chamber, the sensor was screwed-in horizontally and the heater side was facing the flow. The gas flow of 500 ml/min consisted of 2 % H_2O, 3 % CO_2, 10 % O_2. Nitrogen was used as the carrier gas for all experiments. To poison the sensor, 250 ppm SO_2 were added for 1 hour. Three sensors were poisoned with sulfur dioxide: two at 600 °C and one at 800 °C. The sensor resistance R_0 was measured in a 4-wire configuration using a Keithley 2700 digital multimeter (Keithley Instruments, Cleveland, OH, USA). As in other studies, the relative change in resistance (in %) (also called relative signal amplitude) was analyzed to allow comparison between sensor elements of different thicknesses:

$$\frac{\Delta R}{R_0} = \frac{R - R_0}{R_0} \tag{2-1}$$

with the reference resistance R_0. As mentioned above, this study also aims to investigate the possibility of regenerating the $BaFe_{0.74}Al_{0.01}Ta_{0.25}O_{3-\delta}$ films by thermal treatment (similar to NO_x storage catalysts). However, as BFAT only exhibits *p*-type behavior in oxidizing atmospheres and its electrical resistance is temperature independent under these conditions only, the material is primarily intended for lean-burn engines. Therefore, thermal treatment is investigated in oxidizing atmospheres. For this purpose, one of the sensors poisoned with SO_2 at 600

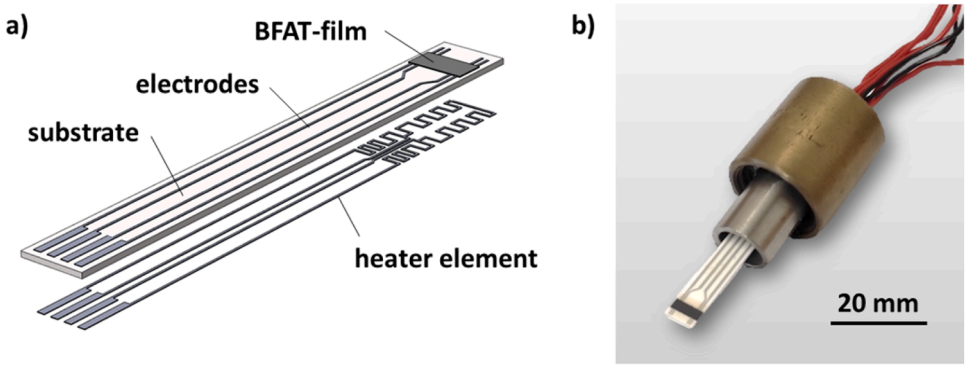

Fig. 1. (a) schematic sensor layout of the resistive sensor elements with the $BaFe_{0.74}Al_{0.01}Ta_{0.25}O_{3-\delta}$ film and (b) illustration of the contacted sensors in the housing.

°C was heated up to 900 °C (3 K/min) in a chamber furnace in synthetic air. The dwell time at 900 °C was 20 min. Additionally, the 4-wire resistance of the BFAT film was measured during the thermal treatment. The same experiment was also performed with a fresh sensor element to derive conclusions about a possible regeneration during the experiment.

The analysis of the sensor properties (oxygen and cross-sensitivities) of the poisoned sensors were conducted using actively heated sensors. Therefore, the two sulfurized sensors (600 °C and 800 °C), the thermally treated sensor, and a fresh sensor were all operated at an operating temperature of 600 °C. The orientation of the sensor within the flow were identical to those employed in the poisoning experiment. First, the response of the sensors to the pO_2 was measured. For this purpose, the pO_2 in the gas flow (6 l/min, with 2 % H_2O, 3 % CO_2, balance N_2) was varied in the range of 20 mbar $\leq pO_2 \leq$ 200 mbar (2 kPa $\leq pO_2 \leq$ 20 kPa, corresponding to approximately $1.1 \leq \lambda \leq 6$).

Then, the cross-sensitivities to typical pollutants were analyzed such as NO, CO, H_2, NO_2, C_3H_8 and NH_3 (6 l/min, with 2 % H_2O, 3 % CO_2 and 20 % O_2, balance N_2). To compare the effects of sulfurization on the selectivity with the results of fresh sensors, the procedures and conditions were adopted from an experiment, that was performed in [19]. In this previous study, a sensor temperature of 750 °C was used and fresh sensors were found to be highly selective to oxygen. This general observation was hardly affected by temperature. Although the operating temperatures is slightly different from the initial condition of this study, the experiment will still allow conclusions to be drawn about the general effects of poisoning on selectivity as well as a qualitative classification of the sensor responses.

In the study, the formation of sulfates was also analyzed to derive conclusions about the mechanisms of sulfur poisoning of the sensor film. A first investigation attempted to detect the poisoning by crystallographic means using X-ray diffraction (Bruker D8 Advance, Billerica, MA, USA, with 2.2 kW Cu anode, $K_{\alpha 1}$ wavelength of 1.540 Å germanium $K_{\alpha 1}$ monochromator and energy dispersive 1D-LYNXEYE detector). The X-ray diffraction patterns were investigated in the range $2\Theta = 20° - 80°$ with an angular resolution of 0.05°. The lattice properties were also derived using Rietveld refinement (DIFFRAC.SUITE TOPAS). Initially the poisoned BFAT sensor films themselves were analyzed. In a second step, powder samples, which were exposed to harsher sulfurization conditions, were investigated by XRD as well. For this purpose, the powder was exposed to SO_2 on a porous quartz frit of a vertical furnace chamber at a temperature of 800 °C. The gas flow was again 500 ml/min with 2 % H_2O, 3 % CO_2 with 10 % O_2 in N_2. To maximize the poisoning effect, the SO_2 treatment (250 ppm) was extended to 4 h. The focus here was on the general identification of sulfate compounds on the material and their structural confirmation.

To detect sulfates on the BFAT sensor film surface as well, X-ray photoelectron spectroscopy (XPS) was used instead, analyzing binding energies up to 1.1 keV. A PHI 5000 VersaProbe III photoelectron spectrometer (Physical Electronics, Feldkirchen, Germany) with an Al K_α source (1486.6 eV) and a quartz crystal monochromator was used in the experiment. The spectral resolution was 0.1 eV.

3. Results

First, the resistive sensor response to sulfur exposure (250 ppm, 1 h) of the sensor elements was analyzed. Fig. 2 shows the relative change in the electrical resistance $\Delta R/R_0$ at an operating temperature of 600 °C (black) and 800 °C (blue). The resistances of the sensor films increase rapidly at the beginning of the SO_2 exposure. At 800 °C, the sensor signal shifts to higher values only for the first 30 min and stagnates for the rest of the experiment. Nevertheless, the resistance changes by almost an order of magnitude from approx. 7.5 kΩ (fresh) to approx. 70 kΩ. Even after the SO_2 dosing was stopped, the sensor signal remains almost unchanged (with a very weak downward trend). The effect of poisoning is even more significant at 600 °C. Here, the sensor signal increases throughout the experiment, which continues beyond the SO_2 dosing. This indicates that sensor poisoning at 600 °C continues after dosing, probably initiated by adsorbed sulfates. Overall, the electrical resistance increases by more than a decade from approx. 10 kΩ in the fresh state to over 150 kΩ. Sulfur dioxide poisoning obviously has a greater effect at lower sensor temperatures.

Nevertheless, even at 800 °C, the effects on the BFAT material are still enormous. In general, the poisoning resistance of the BFAT film to sulfur poisoning appears to be low. Also, some important differences to STF can be seen: At 600 °C, changes of only ca. 10–20 % were measured for STF, largely due to sulfates adsorbed on the surface. However, at higher temperatures (> 700 °C), STF decomposition is increasingly activated [27]. Then, the effects of sulfur poisoning between STF and BFAT are quantitatively quite similar, suggesting that sulfurization even

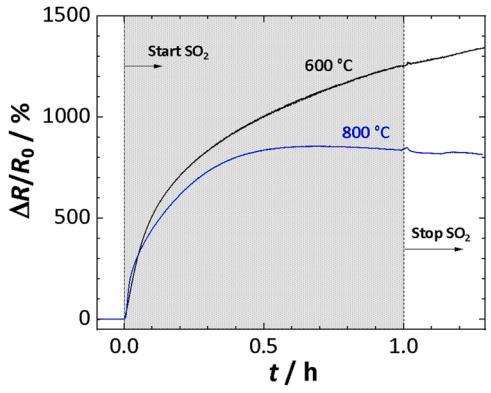

Fig. 2. Relative signal amplitude of the BFAT sensor films during poisoning experiment with SO_2 (250 ppm, 1 h) at sensor temperatures of 600 °C (black, R_0 = 9.8 kΩ) and 800 °C (blue, R_0 = 7.5 kΩ).

of a dense BFAT film is not only limited to surface poisoning. Another difference is also observed. For STF, decomposition increases significantly with temperature with strong effects on the sensor signal. For BFAT the effect is reversed. Here the relative sensor resistance is less affected at higher temperatures (Fig. 2).

Another important question is whether the poisoning can be completely or at least partially reversed by treating the sensor in oxidizing atmospheres at higher temperatures. For this purpose, the sensor element poisoned at 600 °C was heated up to 900 °C in a chamber furnace and was electrically analyzed during heating and cooling. The effects of the experiment on the conductivity σ of the sulfurized BFAT sensor film are shown in Fig. 3 (blue). For comparison, the typical curve of a fresh sensor element is also shown (black). It shows little differences in conductivity during heating and cooling and follows essentially the same curve. Instead, the poisoned sensor shows clear differences. As can be seen in Fig. 3, the conductivity is significantly lower during heating. The approximately 1.5 orders of magnitude correspond to the results from the poisoning of the sensor element (Fig. 2). In addition, two processes can be observed during heating, which are not present in the fresh sensor. The first occurs at just above 600 °C, where the conductivity drops briefly. Above 800 °C, a second effect results in a noticeable and permanent increase in conductivity for a little less than a decade.

The final temperature of 900 °C is held for 20 minutes. The unchanged conductivity at the maximum temperature shows that no further regeneration of the sensor conductivity can be expected by simply extending the dwell time. However, this might be possible at even higher temperatures. At the same time, however, the thermal stress on the sensor element and the sensor film increases. Such conditions, whether induced by the exhaust gas or by active sensor heating, are not desirable. Therefore, this will not be investigated beyond this point in our study. During cooling, the sulfurized sensor now shows a higher conductivity. The conductivity is still below of that of a fresh sensor element. However, similar trends can be observed during cooling. The conductivities of the two sensor films even increasingly converge, especially at low temperatures (< 500 °C). Overall, only a partial regeneration of the film conductivities can be observed. Complete regeneration is obviously not achieved under these conditions.

From a sensor perspective, it is also important to understand how sulfur poisoning affects the sensitivity of the sensor elements. In this context, Fig. 4 shows the sensor signals at different oxygen concentrations (sensor temperature 600 °C). The relative change in resistance at different oxygen stoichiometries (reference resistance R_0 at $\lambda = 6$) is shown in Fig. 4a and the corresponding sensor film conductivities versus pO_2 are depicted in Fig. 4b. Both figures compare the poisoned sensors (blue, red, green) with the properties of a fresh sensor element (black). The signal of the fresh sensor is of a similar order of magnitude as in [19], where the operating temperature was slightly different. Fig. 4a and b show that the electrical resistance of the BFAT films generally increases with lower oxygen stoichiometry and therefore the conductivity σ increases with higher pO_2, which is typical for the *p*-type conducting nature of the barium-iron-tantalate (BFT) family [23].

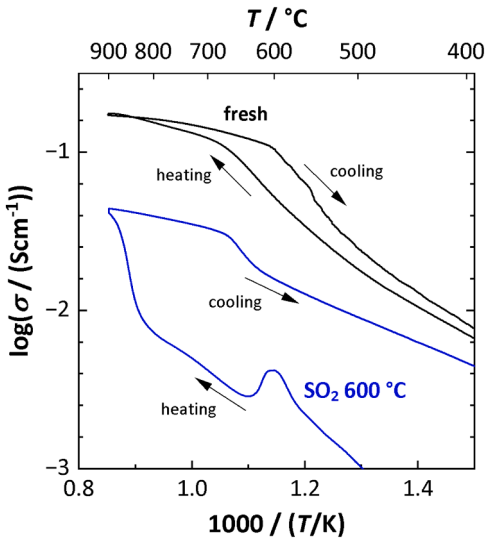

Fig. 3. Conductivities of the fresh (black) and the poisoned (at 600 °C, blue) BFAT sensor film over $1/T$ during the thermal treatment up to 900 °C.

It is also noticeable in Fig. 4a that the changes in the relative signal amplitude increase more towards atmospheres with less oxygen excess i.e., slightly lean oxygen stoichiometries (close to $\lambda = 1$). This effect can be explained by the fact that the pO_2 changes significantly more under these conditions and therefore, this behavior is typical for resistive metal oxide sensors whose defect equilibrium depends on the oxygen concentration in the ambience. At the same time, Fig. 4b shows that the change in conductivity with pO_2 (in a double logarithmic representation) is linear, which is also expected from defect chemistry and will be analyzed in more detail in the following.

Multiple effects of SO_2 poisoning are evident when comparing the data:

1. The sensor signals (relative change in resistance) of the sulfurized sensors to changes in oxygen stoichiometry are significantly lower (Fig. 4a). The lowest sensitivity in this respect is observed for the sensor poisoned at 600 °C (blue), which shows about 27 % of the signal amplitude of a fresh sensor (black). At the same time, the signal amplitude of the sensor increases again after the temperature treatment (green), which also indicates a partial regeneration of the sensor material. The amplitudes are then comparable to those of the sensor poisoned at 800 °C (red). However, they are still only about half those of a fresh sensor.

2. This classification is also confirmed by the different conductivities (Fig. 4b). In line with previous results, the conductivities of the poisoned sensors are significantly lower. The sensor sulfurized at 600 °C (blue) has the lowest conductivity (about 1.5 decades compared to the fresh sensor). The (partially) regenerated sensor (green) and the sensor that was sulfurized at 800 °C (red) have similar conductivities.

3. The pO_2-dependencies of the conductivities, detailed listed in Table 1, also show a similar picture. The fresh sensor has a pO_2-dependence of around +1/4. This value is typical for BFAT and is based on the formation of defect electrons $h^\bullet$ due to the filling of oxygen vacancies in the lattice [23–25]. Deviations are probably mainly due to the sensor temperature of 600 °C. Studies have shown that sensor temperatures above 700 °C are more favorable, since only then the resistivity of this BFAT composition is fully temperature independent [19,21]. Compared to the fresh sensor, pO_2-dependencies of the poisoned sensors are significantly lower. Again, the dependencies of the post-treated sensor and the sensor poisoned at 800 °C are similar, the sensor poisoned at 600 °C shows the smallest pO_2-dependence. Overall, the evaluation of sensor sensitivity gives a consistent picture of the effects on the relative resistance amplitude, electrical conductivity, and their pO_2-dependencies.

In the next step the selectivity of the sensors is evaluated. Gaseous components that are typically found in exhausts are considered. The result of the experiment to analyze the cross-sensitivities is shown in Fig. 5. The relative signal amplitude of a fresh sensor is again shown in black. As can be seen from the figure, new sensors typically have no or very low cross sensitivities. This has already been confirmed by previous measurements in [19], where a similar experiment was performed at a sensor temperature of 750 °C. In contrast, the poisoned sensors show significant responses to different gases. Cross sensitivities are mainly observed for propane and NO_2, and to a lesser extent also for NO and ammonia. As in the fresh state, the sensor signals remain largely independent of CO and H_2. Consistent with previous results, the strongest effect of SO_2 poisoning is again observed for the sensor that was sulfurized at 600 °C (blue). In particular, its signal amplitudes to oxygen stoichiometry λ and to typical concentrations of emissions are of similar

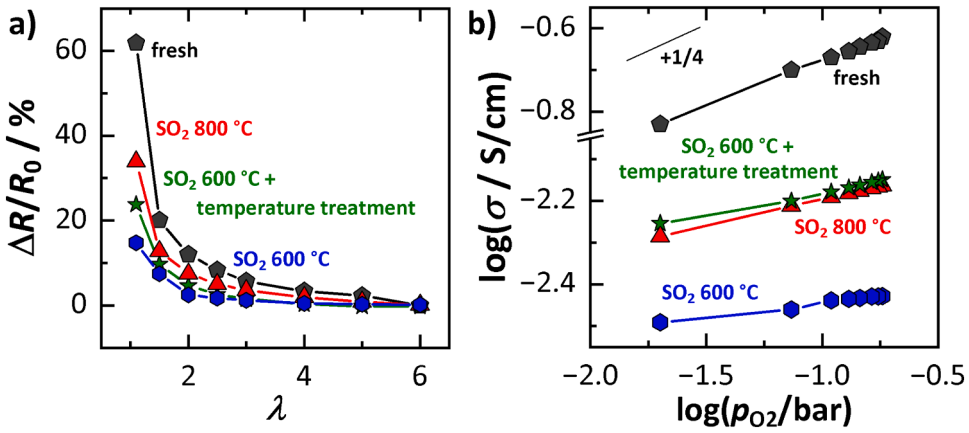

Fig. 4. (a) relative signal amplitudes over the oxygen stoichiometry λ and (b) pO_2-dependent conductivities of the fresh (black) and the poisoned sensors (colored) at an operating temperature of 600 °C.

Table 1
Comparison of pO_2^m-dependences (range: 20 mbar $\leq pO_2 \leq$ 200 mbar) of the fresh and the poisoned BFAT sensor films.

Sensor	pO_2^m-dependence m
fresh	1/4.69
SO_2 600 °C	1/14.3
SO_2 600 °C + temp. treatment	1/9.09
SO_2 800 °C	1/7.88

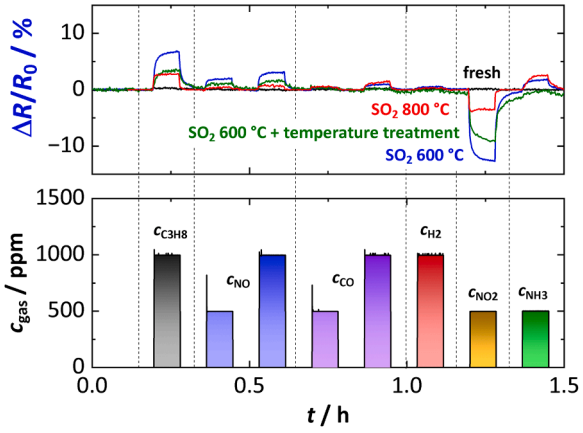

Fig. 5. Analysis of the cross-sensitivities of the BFAT sensor films with (a) the relative signal amplitude and (b) the gas concentrations during the experiment. Sensor temperature: 600 °C.

magnitude (considering the response to propane and NO_2). In principle, a reliable determination of the oxygen concentration with poisoned sensors under dynamic exhaust gas conditions is questionable based on these findings.

A temperature treatment at 900 °C (green) reduces the cross-sensitivities somewhat but does not significantly improve the result. Sulfur poisoning at higher temperatures (800 °C, red) leads to the smallest increase in cross-sensitivities but is only marginally better than the post-treated sensor in terms of NO_2 cross-sensitivity. In this respect, the combination of lower sensitivity and greatly reduced selectivity is critical for operation and remains a key problem for BFAT-based sensors in the field of application. And although the SO_2 concentration of 250 ppm in the experiment was extremely high, it can be assumed that exposure to lower concentrations should have similar effects on the sensor material in the long term. Therefore, the development of BFAT sensor films with higher sulfur resistance is essential in the future.

Based on the previous investigations, it is therefore important to understand how the poisoning affects BFAT from the material perspective. Therefore, the sensor films were also analyzed by X-Ray diffraction. Their diffraction patterns confirmed the perovskite phase of the BFAT films (with broad reflections due to its nanocrystalline morphology). Rietveld analysis suggests crystallite sizes of about 20 nm, which is in line with previous findings [19,21]. Besides the reflections of the Al_2O_3 substrate underneath the sensor layer, no other secondary phases and therefore no sulfates were detected in the diffraction pattern of the film. This result suggests that the quantitative amount of sulfates at the dense sensor film is low (typically below the resolution limit of 1–2 % for XRD measurements) and that sulfate formation might be limited to surface-near regions than rather in the deeper bulk material. Because of this finding and for a generally identification of sulfate compounds and their structural properties, the poisoning was forced even stronger on the starting BFAT powder (as described above). The result of the XRD analysis is shown in Fig. 6, wherein Fig. 6a gives an overview of the main reflection angles of poisoned powder that originate exclusively from BFAT [19,21].

However, for the powder also secondary reflections of lower intensity can be observed, which are shown in detail in Fig. 6b. Their diffraction angles can be assigned to the crystal structure of the barium

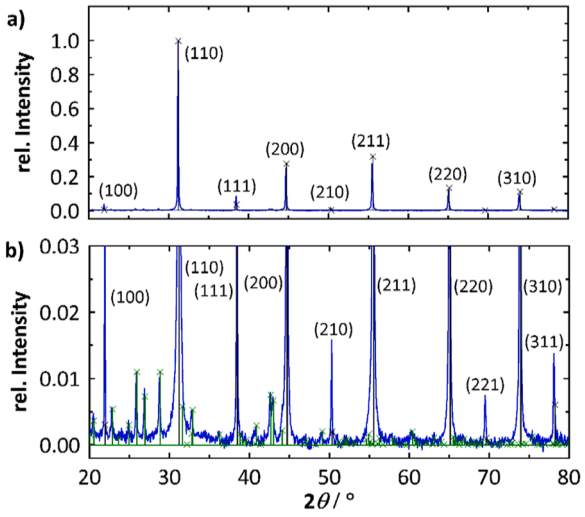

Fig. 6. X-Ray diffraction patterns of the powder poisoned at 800 °C: (a) Overview with the typical diffraction angle of the BFAT perovskite (black, [21, 45,46]), (b) detailed view with additional diffraction angles of barium sulfate (green, [47,48]).

sulfate that was formed during SO_2 exposure. The lattice parameters and crystalline properties of the BFAT powder and $BaSO_4$ were identified by Rietveld refinement. Table 2 shows details of this analysis. The percentage of barium sulfate in the sulfurized powder was quantified to be around 10 %. It should be noted that due to the different morphology of the loose powder and the dense nanocrystalline PAD film on the sensor, the result on the powder cannot be directly extrapolated to the sensor application. The amount of $BaSO_4$ in the dense BFAT sensor film is likely to be lower. However, the main focus of this analysis was to confirm the formation of sulfates in general, which is clearly visible in the X-ray diffractogram. Furthermore, since the environmental conditions in the sulfurization experiments are similar, we can conclude that the poisoning mechanism in the powder and the film will be identical. Incidentally, the structural analysis of a powder sample that had previously been sulfurized at 600 °C (250 ppm SO_2, 4 h) showed the same results, but the percentage of $BaSO_4$ was only 3–4 %.

To finally confirm the formation of sulfates on the sensor film, both the fresh sensor element and the sensor element poisoned at 600 °C were analyzed by XPS. An overview of the binding energy spectrum of both samples is shown in Fig. 7, with the spectrum of the fresh sensor shown in Fig. 7a. The typical energy levels of the Ba, Ta, Fe and O orbitals are determined. The material also contains 1 % Al whose binding energies E_b (1 s, 2 s, 2p orbitals) are barley appear in the spectrum due to the small amount in the BFAT composition. Compared to the fresh state, the poisoned sensor element has additional energy levels, marked in red in Fig. 7b, which are typical for the 2 s and 2p orbitals of sulfur. The corrected sulfur 2p orbital (Fig. 7c) was detected at $E_b = 169.1$ eV (carbon 1 s, $E_b = 285.0$ eV). This value is characteristic for metal oxide sulfates and has been measured in a very similar way in other XPS studies on $BaSO_4$ [48–50]. We can therefore assume, that barium sulfate is indeed present in the near surface region. A comparison between the poisoned and the fresh sensor film (Fig. 7a and b) also shows that after the sulfurization the Ba energies are intense while those of Ta and Fe become weaker. This could be interpreted as another indication that more Ba (preferably in the form of sulfates) is present at the surface.

4. Discussion

The effects of SO_2 on the electrical properties of perovskites of the BFT family are poorly described in the literature. In this section, some ideas on poisoning and possible mechanisms are discussed, taking into account the results shown above and findings from the literature on related materials. The introduced models serve as initial explanatory approaches, but require further verification through additional investigations. This study is not intended to provide a complete description of the mechanisms of poisoning, as the experimental focus is on the analysis of the sensor effects of sulfur poisoning.

Two mechanisms are known in the poisoning of metal oxides with sulfur dioxide. The first one is the adsorption and formation of sulfates on the surface, which is favored at low temperatures. The adsorption of sulfates on the surface of barium materials and perovskites is well documented [36]. It follows a mechanism that has been found to be similar in STF [27]:

$$SO_2(g) + 2O^x_{O,Surface} + 2h^\bullet \leftrightharpoons (SO_4)^x_{O,Surface} + V^{\bullet\bullet}_{O,Surface} \quad (4\text{-}1)$$

The formation of sulfates at the grain boundaries consumes two defect electrons with the formation of additional oxygen vacancies. The adsorption of sulfates therefore leads to a depletion of the defect electron concentration accompanied by the formation of a space charge zone in the crystal. Although it is clear that the concentration of charge carriers will decrease, particularly in the areas close to the surface, it should be noted that this effect will have a greater impact on sensor elements using porous sensor films due to the larger surface area. Accordingly, the effect should be weaker for dense BFAT-PAD films

Furthermore, the thermal treatment has shown that poisoning of the BFT sensor material is reversible, at least partially, i.e. the increase in resistance can be reversed (Fig. 3). It can be assumed that this is mainly due to the sulfates on the surface, which can be (partially) removed during the thermal treatment. In fact, the properties of the sensor sulfurized at higher temperatures were largely identical to those of the sensor poisoned at low temperatures and then regenerated. As is known from the literature, these surface-bound sulfates are largely easy to remove, whereas bulk barium sulfates are difficult to reduce (and even more under oxidizing conditions).

At the same time, XRD and XPS measurements on the powder and the film (Figs. 6 and 7) show that bulk $BaSO_4$ is formed during the poisoning process, which confirms that the incorporation of sulfur into deeper lattice layers also occurs. Therefore, Ba cations from the perovskite are chemically bound as sulfates, which raises the question of how this affects the remaining cations of the perovskite. Analogous to STF, the Fe and Ta cations precipitate as (mixed) oxides. Due to the different cation stoichiometries between the perovskite and the metal oxides, it is also likely that the composition of the perovskite is locally affected, i.e. a different ratio of iron and tantalum is induced in the surrounding perovskite lattice. In this respect, it is also known from BaFe perovskites for NSC applications that in particular iron is converted into iron(III) sulfate [41]. This mechanism is even intended to suppress the alternative formation of barium sulfate and to simplify the desulfurization of iron sulfates. However, the amount of $Fe_2(SO_4)_3$ is highly dependent on the crystalline order of the perovskite [40,41]. It can be assumed here that the dense nanocrystalline structure of the PAD films could be disadvantageous. In fact, studies have shown that the formation of barium sulfate is favored primarily along grain boundaries [38]. Determining the exact mechanisms that take place at the sensor during sulfur poisoning is not trivial. One reason is the fact that, due to the stoichiometry of the reaction, the amount of oxides formed is less than the amount of $BaSO_4$ formed (typically not higher than a factor of ½). The ratio of formed oxides to barium sulfate is typically not higher than a factor of ½ and can be followed by reaction stoichiometry. For example: Assuming a complete decomposition of BFT (ignoring the small amount of aluminum for simplicity) to iron(III)oxide (Fe_2O_3), its chemistry follows Eqn 4-2 (similar to a mechanism introduced in [27]):

$$BaFe_{0.75}Ta_{0.25}O_{3-\delta} + nO_2 + 0.75SO_4(g) \leftrightharpoons 0.75BaSO_4 + 0.25BaTaO_{3-\delta'} + 0.375Fe_2O_3 \quad (4\text{-}2)$$

with the oxygen deficiencies δ of BFT and of the iron-depleted barium tantalate δ' and the amount of oxygen n to balance the equation. Following this mechanism, the ratio between iron oxide and barium sulfate formed during poisoning is 0.375/0.75 = ½. The same factor can be derived for a decomposition into tantalum oxide. These numbers change only slightly when aluminum (content 1 %) is considered. This shows that the amount barium sulfate is higher than those of formed oxides by a factor of ca. 2. At the same time, the orthorhombic structure of $BaSO_4$ has many diffraction angles in the pattern that overlap partially those of possible oxide products. Both factors make an identification of secondary phases quite challenging and might explain why besides BAFT and sulfates no other phases were found in the diffraction

Table 2
Results of the Rietveld refinement of the powder with the perovskite-structure of BFAT and the orthorhombic barium sulfate.[1].

Material	$BaFe_{0,74}Al_{0,01}Ta_{0,25}O_3$		$BaSO_4$	
Concentration	ca. 90 %		ca. 10 %	
Spacegroup	Pm-3m		Pnma	
Lattice constants	*a* / Å	4.03917(8)	*a* / Å *b* / Å *c* / Å	8.879(3)5.463(3)7.157(4)
Crystallite size	197.3 nm		78.9 nm	
Residual Fit Error	9.764 %			

[1]The numbers in brackets represent the uncertainties in the last digits of the lattice parameters.

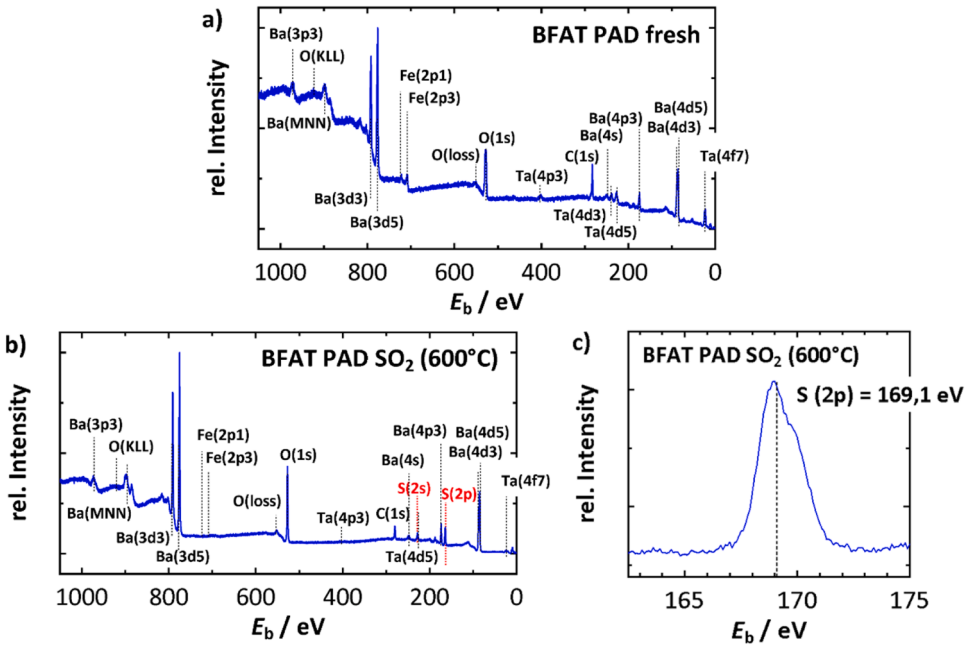

Fig. 7. X-ray Photoelectron spectra of (a) the fresh sensor film with the typical binding energies of Ba, Ta, Fe and O and (b) the poisoned sensor film with additional energies of sulfur (highlighted red). (a) detailed view of the energy maxima at the S(2p) orbital at 169,1 eV.

measurements.

However, the question remains whether these mechanisms described in the literature can also explain the impact on the electrical properties in the BFAT film. Here, the measurements showed a significant increase in electrical resistance with proceeding sulfurization (Fig. 2). In addition to the insulating effect of bulk sulfates and (potential) oxides, the favored formation of iron sulfates (or oxides) in particular has an additional effect: Sulfur poisoning (similar to STF [27]) could then lead to iron-deficient perovskites. Previous studies on different compositions have shown that higher Ta concentration reduces the conductivity of BFAT, because Ta (assumed to be in the 5+ state) acts as a donor in the perovskite [21,51]. At the same time, the process may affect the sensitivity towards oxygen of the material. For stoichiometric tantalum contents $>$ 40 %, the pO_2 dependence drops to +1/5 and is almost insensitive to pO_2 at $>$ 45 % [51]. Based on these mechanisms, both a reduced conductivity and a lower response to pO_2 changes (or oxygen stoichiometry changes) is expected (Fig. 4). Furthermore, combining the insulating character of both weakly bound surface sulfates and chemical more stable bulk sulfates might also explain the results during the thermal treatment. When a poisoned (600 °C) sensor is heated up to higher temperatures, the electrical conductivity of BFAT could then by partially restored by removing surface sulfates and the recovery of the defect electrons in BFAT.

Another question that remains unanswered is why the selectivity of the sensor layer decreases so much (see Fig. 5). While fresh sensors react almost exclusively to oxygen, significantly increased cross-sensitivities to many gases can be detected after poisoning. Again, this could be caused by the significant decrease in electrical conductivity ($>$ decade) during poisoning. Since the relative amplitude in electrical resistance is used as a sensor signal (not conductivity!), even smaller (absolute) changes in the majority charge carriers have a greater impact on the relative changes in electrical properties at the reduced conductivity levels. Assuming interfering gases affect fresh and poisoned sensors to a similar extent, the cross-sensitivities should increase with poisoning. It is also possibly, that sulfates might also promote interaction to specific gases to some extent. However, further investigations are required regarding this topic, which is beyond the scope of this work.

However, an effect was observed during poisoning of BFAT sensor films that is fundamentally different from the results for STF: For STF, decomposition was observed at temperatures above 600 °C. Here, the kinetics of poisoning and the effect on the electrical resistance increase rapidly with higher temperatures. Although an increased formation of barium sulfates with higher temperatures was also observed for BFAT (confirmed by diffraction pattern of powders), the effect of poisoning on the sensor signal is less at 800 °C (Fig. 2). In this regard, the combination of adsorption and sulfate formation has a greater influence on the sensor properties at low temperatures. At the same time, despite higher temperatures, the poisoning of bulk material is probably still limited to the upper lattice films, while the incorporation of sulfates in deeper bulk regions, might be progressively decelerated. As a result, the overall electrical properties of the film could be less affected by poisoned structures (despite larger quantities) at high temperatures. In order to understand this effect in more detail, further investigations on sensors films with different thicknesses would be recommended. An analysis of the progression of sulfur poisoning in the bulk material using XPS (sputter) depth profiling could also provide valuable information. However, both are beyond the scope of this study.

For the sensor application the results suggest that higher sensor temperatures (750–800 °C) should be preferred since the impact on conductivity, sensitivity and selectivity is lower at these conditions, despite possibly forming more sulfates. Since the formation of sulfates in deeper layers is kinetically suppressed, a thicker sensor film might also be less affected by SO_2 poisoning and provide better sulfur resistivity. Nevertheless, although the sulfur concentrations used in the experiment are quite high (compared to expected concentrations in exhaust gases), the sulfur resistance of BFAT remains a challenge from the sensor perspective. Still, other solutions like the integration of a SO_2 absorber as a protective layer might be worth to be investigated.

5. Conclusions

This study presents an investigation of SO_2 exposure of dense BFAT sensor films for oxygen sensing applications. The measurements have shown that the SO_2 exposure has a significant effect on the electrical properties of the material and thus also on the sensing capabilities. In addition to an increase in resistance, the sensitivity to oxygen is reduced. At the same time, the selectivity of the sensor is negatively affected. The combination of these effects leads to a significant reduction in signal

quality and, hence, SO_2 poisons the BFAT films and makes their application in SO_2 containing exhausts questionable. In conclusion, strategies to increase the sulfur resistance of the sensor films are needed. Experiments on the poisoned material (XRD, XPS) have confirmed the formation of $BaSO_4$ in particular. Regeneration of poisoned sensor films is only partially possible under oxidizing conditions, but will most likely only remove surface adsorbed sulfates rather than bulk barium sulfates.

Funding

This research was granted by the Deutsche Forschungsgemeinschaft (DFG), DFG Grant MO 1060/41–1.

CRediT authorship contribution statement

Carsten Steiner: Writing – review & editing, Writing – original draft, Visualization, Validation, Software, Methodology, Investigation, Conceptualization. **Gunter Hagen:** Writing – review & editing, Validation, Supervision, Methodology, Conceptualization. **Ralf Moos:** Writing – review & editing, Validation, Supervision, Methodology, Conceptualization.

Declaration of Competing Interest

The authors declare that they have no known competing financial interests or personal relationships that could have appeared to influence the work reported in this paper, Ralf Moos reports a relationship with German Research Foundation that includes: funding grants. If there are other authors, they declare that they have no known competing financial interests or personal relationships that could have appeared to influence the work reported in this paper.

Acknowledgments

The authors are indebted to the Department of Metals and Alloys (Prof. Uwe Glatzel), University of Bayreuth for XRD measurements. The access to the XPS/UPS facility (PHI 5000 VersaProbe III system) at the Device Engineering KeyLab in the Bavarian Polymer Institute, University of Bayreuth is gratefully acknowledged. We also thank W. Reichstein for his expertise on the device.

Statement

During the preparation of this work the authors used DeepL Write in order to improve the readability and language of the manuscript. After using this tool, the authors reviewed and edited the content as needed and take full responsibility for the content of the published article.

Data availability

Data will be made available on request.

References

[1] J. Gerblinger, M. Hausner, H. Meixner, Electric and kinetic properties of screen-printed strontium titanate films at high temperatures, J. Am. Ceram. Soc. 78 (1995) 1451–1456, https://doi.org/10.1111/j.1151-2916.1995.tb08836.x.
[2] T.S. Stefanik, H.L. Tuller, Ceria-based gas sensors, J. Eur. Ceram. Soc. 21 (2001) 1967–1970, https://doi.org/10.1016/S0955-2219(01)00152-2.
[3] R. Moos, N. Izu, F. Rettig, S. Reiss, W. Shin, I. Matsubara, Resistive oxygen gas sensors for harsh environments, Sensors 11 (2011) 3439–3465, https://doi.org/10.3390/s110403439.
[4] P.T. Moseley, D.E. Williams, Gas sensors based on oxides of early transition metals, Polyhedron 8 (1989) 1615–1618, https://doi.org/10.1016/S0277-5387(00)80606-3.
[5] C. Argirusis, F. Jomard, S.F. Wagner, W. Menesklou, E. Ivers-Tiffée, Study of the oxygen incorporation and diffusion in $Sr(Ti_{0.65}Fe_{0.35})O_3$ ceramics, Sol. St. Ion. 192 (2011) 9–11, https://doi.org/10.1016/j.ssi.2010.02.016.
[6] N. Izu, W. Shin, I. Matsubara, T. Itoh, M. Nishibori, N. MURAYAMA, Pt catalytic effects on a resistive oxygen sensor using $Ce_{0.9}Zr_{0.1}O_2$ thick film in rich conditions, J. Ceram. Soc. Jpn. 118 (2010) 175–179, https://doi.org/10.2109/jcersj2.118.175.
[7] N. Izu, S. Nishizaki, W. Shin, T. Itoh, M. Nishibori, I. Matsubara, Resistive oxygen sensor using ceria-zirconia sensor material and ceria-yttria temperature compensating material for lean-burn engine, Sensors 9 (2009) 8884–8895, https://doi.org/10.3390/s91108884.
[8] T. Mun, J.Y. Koo, J. Lee, S.J. Kim, G. Umarji, D. Amalnerkar, W. Lee, Resistive-type lanthanum ferrite oxygen sensor based on nanoparticle-assimilated nanofiber architecture, Sens. Actuators B Chem. 324 (2020) 128712, https://doi.org/10.1016/j.snb.2020.128712.
[9] G. Neri, G. Micali, A. Bonavita, R. Licheri, R. Orrù, G. Cao, D. Marzorati, E. Merlone Borla, E. Roncari, A. Sanson, $FeSrTiO_3$-based resistive oxygen sensors for application in diesel engines, Sens. Actuators B Chem. 134 (2008) 647–653, https://doi.org/10.1016/j.snb.2008.06.007.
[10] R. Ranga, A. Kumar, P. Kumari, P. Singh, V. Madaan, K. Kumar, Ferrite application as an electrochemical sensor: A review, Mater. Charact. 178 (2021) 111269, https://doi.org/10.1016/j.matchar.2021.111269.
[11] A. Stratulat, B.-C. Serban, A. de Luca, V. Avramescu, C. Cobianu, M. Brezeanu, O. Buiu, L. Diamandescu, M. Feder, S.Z. Ali, et al., Low Power Resistive Oxygen Sensor Based on Sonochemical $SrTi_{0.6}Fe_{0.4}O_{2.8}$ (STFO40), Sensors 15 (2015) 17495–17506, https://doi.org/10.3390/s150717495.
[12] A.S. Mokrushin, E.P. Simonenko, N.P. Simonenko, K.A. Bukunov, V. G. Sevastyanov, N.T. Kuznetsov, Gas-sensing properties of nanostructured CeO_2-$xZrO_2$ thin films obtained by the sol-gel method, J. Alloy. Compd. 773 (2019) 1023–1032, https://doi.org/10.1016/j.jallcom.2018.09.274.
[13] R. Moos, F. Rettig, A. Hürland, C. Plog, Temperature-independent resistive oxygen exhaust gas sensor for lean-burn engines in thick-film technology, Sens. Actuators B Chem. 93 (2003) 43–50, https://doi.org/10.1016/S0925-4005(03)00333-2.
[14] A. Rothschild, S.J. Litzelman, H.L. Tuller, W. Menesklou, T. Schneider, E. Ivers-Tiffée, Temperature-independent resistive oxygen sensors based on $SrTi_{1-x}Fe_xO_{3-\delta}$ solid solutions, Sens. Actuators B Chem. 108 (2005) 223–230, https://doi.org/10.1016/j.snb.2004.09.044.
[15] K. Park, E.M. Logothetis, Oxygen sensing with $Co_{1-x}Mg_xO$ ceramics, J. Electrochem. Soc. 124 (1977) 1443–1446, https://doi.org/10.1149/1.2133671.
[16] C. Yu, Y. Shimizu, H. Arai, Investigation on a lean-burn oxygen sensor using perwovskite-type oxides, Chem. Lett. 15 (1986) 563–566, https://doi.org/10.1246/cl.1986.563.
[17] H. Nozaki, J. Tanaka, K. Shibata, Oxygen-sensitive resistivity of La_2CuO_4 at high temperatures, Jpn. J. Appl. Phys. 26 (1987) L1881, https://doi.org/10.1143/JJAP.26.L1881.
[18] A.V. Raghu, K.K. Karuppanan, B. Pullithadathil, Highly sensitive, temperature-independent oxygen gas sensor based on anatase TiO_2 nanoparticle grafted, 2D mixed valent VO x nanoflakelets, ACS Sens 3 (2018) 1811–1821, https://doi.org/10.1021/acssensors.8b00544.
[19] C. Steiner, S. Püls, M. Bektas, A. Müller, G. Hagen, R. Moos, Resistive, temperature-independent metal oxide gas sensor for detecting the oxygen stoichiometry (air-fuel ratio) of lean engine exhaust gases, Sensors 23 (2023) 3914, https://doi.org/10.3390/s23083914.
[20] P.T. Moseley, Solid state gas sensors, J. Mater. Chem. 8 (1997) 223–237, https://doi.org/10.1088/0957-0233/8/3/003.
[21] M. Bektas, D. Schönauer-Kamin, G. Hagen, A. Mergner, C. Bojer, S. Lippert, W. Milius, J. Breu, R. Moos, $BaFe_{1-x}Ta_xO_{3-\delta}$ – A material for temperature independent resistive oxygen sensors, Sens. Actuators B Chem. 190 (2014) 208–213, https://doi.org/10.1016/j.snb.2013.07.106.
[22] M. Schubert, D. Hanft, T. Nazarenus, J. Exner, M. Schubert, P. Nieke, P. Glosse, N. Leupold, J. Kita, R. Moos, Powder aerosol deposition method – novel applications in the field of sensing and energy technology, Funct. Mater. Lett. 12 (2019) 1930005, https://doi.org/10.1142/S1793604719300056.
[23] M. Bektas, T. Stöcker, G. Hagen, R. Moos, On the defect chemistry of $BaFe_{0.89}Al_{0.01}Ta_{0.1}O_{3-\delta}$, a material for temperature independent resistive and thermoelectric oxygen sensors, Sol. St. Ion. 316 (2018) 1–8, https://doi.org/10.1016/j.ssi.2017.12.017.
[24] M. Bektas, T. Stöcker, A. Mergner, G. Hagen, R. Moos, Combined resistive and thermoelectric oxygen sensor with almost temperature-independent characteristics, J. Sens. Sens. Syst. 7 (2018) 289–297, https://doi.org/10.5194/jsss-7-289-2018.
[25] C. Steiner, T. Wöhrl, M. Steiner, J. Kita, A. Müller, H. Eisazadeh, R. Moos, G. Hagen, Resistive Multi-Gas Sensor for Simultaneously Measuring the Oxygen Stoichiometry (λ) and the NOx Concentration in Exhausts: Engine Tests under Dynamic Conditions, Sensors 23 (2023), https://doi.org/10.3390/s23125612.
[26] J. Brettschneider, Extension of the Equation for Calculation of the Air-Fuel Equivalence Ratio, SAE Tech. Pap. (1997) 972989, https://doi.org/10.4271/972989.
[27] F. Rettig, R. Moos, C. Plog, Poisoning of temperature independent resistive oxygen sensors by sulfur dioxide, J. Electroceram. 13 (2004) 733–738, https://doi.org/10.1007/s10832-004-5184-x.
[28] F. Rettig, R. Moos, C. Plog, Sulfur adsorber for thick-film exhaust gas sensors, Sens. Actuators B Chem. 93 (2003) 36–42, https://doi.org/10.1016/S0925-4005(03)00334-4.
[29] F. Rohr, S.D. Peter, E. Lox, M. Kögel, W. Müller, A. Sassi, C. Rigaudeau, L. Juste, G. Belot, P. Gélin, et al., The impact of sulfur poisoning on NO_x-storage catalysts in gasoline applications, SAE Tech. Pap. (2005), https://doi.org/10.4271/2005-01-1113.
[30] E.C. Corbos, X. Courtois, N. Bion, P. Marecot, D. Duprez, Impact of the support oxide and Ba loading on the sulfur resistance and regeneration of Pt/Ba/support

catalysts, Appl. Catal. B 80 (2008) 62–71, https://doi.org/10.1016/j.apcatb.2007.10.009.
[31] S. Elbouazzaoui, E.C. Corbos, X. Courtois, P. Marecot, D. Duprez, A study of the deactivation by sulfur and regeneration of a model NSR Pt/Ba/Al_2O_3 catalyst, Appl. Catal. B 61 (2005) 236–243, https://doi.org/10.1016/j.apcatb.2005.05.012.
[32] F. Rohr, U. Göbel, P. Kattwinkel, T. Kreuzer, W. Müller, S. Philipp, P. Gélin, New insight into the interaction of sulfur with diesel NOx storage catalysts, Appl. Catal. B 70 (2007) 189–197, https://doi.org/10.1016/j.apcatb.2005.12.033.
[33] X. Wei, X. Liu, M. Deeba, Characterization of sulfated BaO-based NOx trap, Appl. Catal. B 58 (2005) 41–49, https://doi.org/10.1016/j.apcatb.2004.04.021.
[34] D.H. Kim, J.H. Kwak, J. Szanyi, C.H. Peden, Isothermal desulfation of pre-sulfated Pt-BaO/γ-Al_2O_3 lean NO_x trap catalysts with H_2: The effect of H_2 concentration and the roles of CO_2 and H_2O, Appl. Catal. B 111-112 (2012) 342–348, https://doi.org/10.1016/j.apcatb.2011.10.017.
[35] W.S. Epling, L.E. Campbell, A. Yezerets, N.W. Currier, J.E. Parks, Overview of the Fundamental Reactions and Degradation Mechanisms of NO_x Storage/Reduction Catalysts, Catal. Rev. 46 (2004) 163–245, https://doi.org/10.1081/CR-200031932.
[36] F. Rohr, S.D. Peter, E. Lox, M. Kögel, A. Sassi, L. Juste, C. Rigaudeau, G. Belot, P. Gélin, M. Primet, On the mechanism of sulphur poisoning and regeneration of a commercial gasoline NO_x-storage catalyst, Appl. Catal. B 56 (2005) 201–212, https://doi.org/10.1016/j.apcatb.2004.09.011.
[37] V. Torregrosa-Rivero, M.-S. Sánchez-Adsuar, M.-J. Illán-Gómez, Analyzing the role of copper in the soot oxidation performance of $BaMnO_3$-perovskite-based catalyst obtained by modified sol-gel synthesis, Fuel 328 (2022) 125258, https://doi.org/10.1016/j.fuel.2022.125258.
[38] C. Ge, L. Li, H. Xian, H. Yan, M. Meng, X. Li, Effects of Ti-doping on the NO_x storage and the sulfur resistance of the $BaFe_{1-x}Ti_xO_{3-y}$ perovskite-type catalysts for lean-burn exhausts, Fuel Process Technol. 120 (2014) 1–7, https://doi.org/10.1016/j.fuproc.2013.11.008.
[39] S. Hodjati, K. Vaezzadeh, C. Petit, V. Pitchon, A. Kiennemann, Absorption/desorption of NO_x process on perovskites: performances to remove NO_x from a lean exhaust gas, Appl. Catal. B 26 (2000) 5–16, https://doi.org/10.1016/S0926-3373(99)00143-5.
[40] H. Xian, X. Zhang, X. Li, H. Zou, M. Meng, Z. Zou, L. Guo, N. Tsubaki, Effect of the calcination conditions on the NO storage behavior of the perovskite $BaFeO_3$− catalysts, Catal. Today 158 (2010) 215–219, https://doi.org/10.1016/j.cattod.2010.03.026.
[41] H. Xian, F.-L. Li, X.-G. Li, X.-W. Zhang, M. Meng, T.-Y. Zhang, N. Tsubaki, Influence of preparation conditions to structure property, NO_x and SO_2 sorption behavior of the $BaFeO_{3-x}$ perovskite catalyst, Fuel Process Technol. 92 (2011) 1718–1724, https://doi.org/10.1016/j.fuproc.2011.04.021.
[42] K. Yamazaki, T. Suzuki, N. Takahashi, K. Yokota, M. Sugiura, Effect of the addition of transition metals to Pt/Ba/Al_2O_3 catalyst on the NO_x storage-reduction catalysis under oxidizing conditions in the presence of SO_2, Appl. Catal. B 30 (2001) 459–468, https://doi.org/10.1016/S0926-3373(00)00263-0.
[43] M. Bektas, D. Hanft, D. Schönauer-Kamin, T. Stöcker, G. Hagen, R. Moos, Aerosol-deposited $BaFe_{0.7}Ta_{0.3}O_{3-\delta}$ for nitrogen monoxide and temperature-independent oxygen sensing, J. Sens. Sens. Syst. 3 (2014) 223–229, https://doi.org/10.5194/jsss-3-223-2014.
[44] J. Exner, T. Nazarenus, D. Hanft, J. Kita, R. Moos, What happens during thermal post-treatment of powder aerosol deposited functional ceramic films? Explanations based on an experiment-enhanced literature survey, Adv. Mater. 32 (2020) e1908104, https://doi.org/10.1002/adma.201908104.
[45] A. Dutta, T.P. Sinha, Structural and dielectric properties of $A(Fe_{1/2}Ta_{1/2})O_3$ [A=Ba, Sr, Ca, Mater. Res. Bull. 46 (2011) 518–524, https://doi.org/10.1016/j.materresbull.2011.01.003.
[46] S. Sivakumar, P. Soundhirarajan, A. Venkatesan, C.P. Khatiwada, Spectroscopic studies and antibacterial activities of pure and various levels of Cu-doped $BaSO_4$ nanoparticles, Spectrochim. Acta, Part A 151 (2015) 895–907, https://doi.org/10.1016/j.saa.2015.07.048.
[47] W.A. Crichton, M. Merlini, M. Hanfland, H. Muller, The crystal structure of barite, $BaSO_4$, at high pressure, Am. Mineral. 96 (2011) 364–367, https://doi.org/10.2138/am.2011.3656.
[48] Y. Kou, Y. Wang, J. Zhang, K. Guo, X. Zhang, Z. Yu, X. Song, Nano $BaSO_4$ prepared by microreactor and its effect on thermal decomposition of some energetics, FirePhysChem 2 (2022) 174–184, https://doi.org/10.1016/j.fpc.2021.11.004.
[49] J. Chastain, J.F. Moulder, Handbook of X-ray Photoelectron Spectroscopy: A Reference Book of Standard Spectra for Identification and Interpretation of XPS Data, Perkin-Elmer Corporation, Eden Prairie, Minn., 1992, p. 61. ISBN 0962702625.
[50] P.J. Schmitz, Characterization of the surface of $BaSO_4$ powder by XPS, Surf. Sci. Spectra 8 (2001) 195–199, https://doi.org/10.1116/11.20011203.
[51] M. Bektas, $BaFe_{(1-x)-0.01}Al_{0.01}Ta_xO_{3-\delta}$: A material for temperature independent resistive and thermoelectric oxygen sensors, Shaker-Verlag, Düren (2020). ISBN 978-3-8440-7459-8.

Carsten Steiner, M.Sc.Carsten Steiner was a student intern at the Research and Innovation Center of the Ford Motor Company in Dearborn, MI, USA in 2015. He graduated with the Master's degree from the Fakulty of Engineering Science of the University of Bayreuth in 2016. Since then he worked as a PhD student at the Department of Functional Materials of the same University. Key aspects of his research are the microwave-based state diagnosis of automotive catalysts and novel sensors for exhaust gas aftertreatment purposes. Special attention in his work is also given to the defect chemistry of metal oxide gas sensors and storage materials in washcoats of various catalyst types.

Dr.-Ing. Gunter Hagen Gunter Hagen received the Diploma degree in materials science in 2003 and the PhD degree in 2009 from the University of Bayreuth, Germany. He is permanent member and senior scientist in the department of Functional Materials, dealing with different kinds of gas sensors, novel sensor and catalyst materials (e.g. zeolites), and exhaust gas aftertreatment systems.

Prof. Dr.-Ing. Ralf Moos Ralf Moos received the Diploma degree in Electrical Engineering from the University of Karlsruhe, Germany, in 1989 and the doctoral degree from the same university with a thesis on the influence of donor dopants in strontium titanate on the electrical properties and defect chemical modelling in 1994. From 1995–2001 he was with Daimler AG, in Stuttgart and Friedrichshafen, Germany and was responsible for gas sensing. In July 2001, he was appointed head of the Department of Functional Materials at the University of Bayreuth. Key aspects of the research work at the Department of Functional Materials are mainly inorganic functional materials and polymer-oxide composites and devices and systems that are made thereof. With respect to materials, perovskites, porous framework materials (e.g., zeolites), and ion conductors are in the focus. Application fields encompass chemical sensors, catalysts, and materials for energy conversion and electrical devices. Special attention is given to film and layer technologies. As it is typical for an engineering research department, industrial applicability of the applied techniques and methods is of special importance.